

Pumping of vibrational excitations in a Coulomb blocked suspended carbon nanotube

A. K. Hüttel,^{1,*} B. Witkamp,¹ M. Leijnse,^{2,3,4} M. R. Wegewijs,^{2,3,4} and H. S. J. van der Zant¹

¹*Molecular Electronics and Devices, Kavli Institute of Nanoscience, Delft University of Technology, PO Box 5046, 2600 GA Delft, The Netherlands*

²*Institut für Theoretische Physik A, RWTH Aachen, 52056 Aachen, Germany*

³*Institut für Festkörper-Forschung - Theorie 3 Forschungszentrum Jülich, 52425 Jülich, Germany*

⁴*JARA - Fundamentals of Future Information Technology*

(Dated: June 21, 2024)

Low-temperature transport spectroscopy measurements on a suspended few-hole carbon nanotube quantum dot are presented, showing a gate-dependent harmonic excitation spectrum which, strikingly, occurs in the Coulomb blockade regime. The quantized excitation energy corresponds to the scale expected for longitudinal vibrations of the nanotube. The respective electronic transport processes are identified as cotunnel-assisted sequential tunneling, resulting from non-equilibrium occupation of the mechanical mode. They appear only above a high bias threshold at the scale of electronic excitations of the nanotube. We discuss models for the pumping process that explain this enhancement of the non-equilibrium occupation above this threshold. An interplay of electronic and vibrational degrees of freedom is found to promote absorption of vibrational quanta.

PACS numbers: 63.22.Gh, 73.63.Fg, 73.23.Hk

The coupling of vibrational modes and electronic transport in nanoscale systems and in particular quantum dots is currently the focus of many theoretical [1, 2, 3] and experimental [4, 5, 6, 7, 8] research efforts. In this respect, single wall carbon nanotubes (SW-CNTs) provide a unique mesoscopic system where both bulk beam mechanics [4, 5, 6] and quantization of phonon modes [7, 8] have already been demonstrated. Low-temperature Coulomb blockade spectroscopy on quantum dots formed within the nanotube [9, 10] has led to a well-developed understanding of the electronic structure of SW-CNTs [11, 12, 13]. In suspended SW-CNT quantum dots, transport spectroscopy has also revealed the Franck-Condon effect: the equilibrium position of the nanotube depends on its charge and transitions between different charge states are no longer determined by the electronic transition rates alone. The vibrational spectrum of the nanotube acting as one quantum-mechanical oscillator becomes visible in single electron tunneling (SET) at finite bias. A large electron phonon coupling [7], and first indications of vibrational phenomena in cotunneling have been observed [14].

In this Letter we present low-temperature transport measurements on a suspended CNT quantum dot system. We observe signatures of non-equilibrium population of the quantized mechanical oscillations in the transport spectrum, revealed by cotunnel-assisted sequential electron tunneling (CO-SET). The non-equilibrium occupation is enhanced (“pumped”) by several higher-order tunnel processes. Detailed models are discussed which explain the observations.

The basic geometry of our device is sketched in Fig. 1(a). A highly p⁺⁺ doped silicon wafer, also functioning as back gate, with 500 nm thermally grown oxide

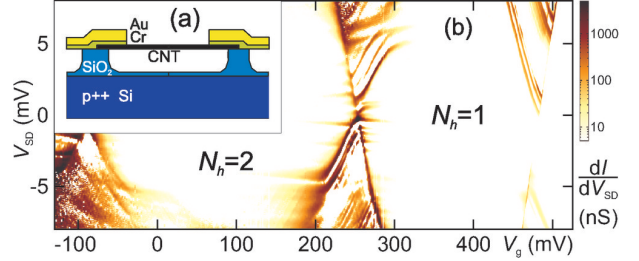


FIG. 1: (Color online) (a) Side view drawing of a typical sample geometry. (b) Overview measurement of the differential conductance dI/dV_{SD} of the nanotube quantum dot system in the few-hole region ($0 \leq N_h \leq 3$) as function of back gate voltage V_g and bias voltage V_{SD} (logarithmic color scale, negative differential conductance is plotted white). In the Coulomb blockade regions, the absolute number of trapped valence band holes N_h is indicated.

on top provides the starting point of the sample preparation. After lithographic fabrication of marker structures and localized deposition of growth catalyst [15], carbon nanotubes are grown in situ by chemical vapor deposition and located using atomic force microscopy. Contact electrodes consisting of 5 nm chromium and 50 nm gold are deposited on top of the nanotubes. In a last step, the nanotube devices are suspended using wet etching in buffered hydrofluoric acid.

Measurements were performed in a dilution refrigerator with a base temperature $T_{MC} \lesssim 20$ mK and an electron temperature $T_{el} \simeq 100$ mK. Fig. 1(b) shows the differential conductance dI/dV_{SD} as function of back gate (substrate) voltage V_g and bias voltage V_{SD} of one particular suspended nanotube quantum dot. This sample has a lithographically designed length of $l = 250$ nm, and

proved to be a semiconducting nanotube with a band gap energy of $E_g = 200$ meV. Band gap energy and device length lead to a predicted energy scale of $\Delta E \simeq 6$ meV of orbital electronic excitations [11]. In the measurement of Fig. 1(b), the basic structure of diamond-shaped Coulomb blockade regions with a fixed trapped charge, as expected for a single quantum dot, is clearly visible. Since the band gap position is known, we can identify the charge states present as $N_h = 1$ and $N_h = 2$, respectively.

Figure 2(a) displays a detail measurement of the SET

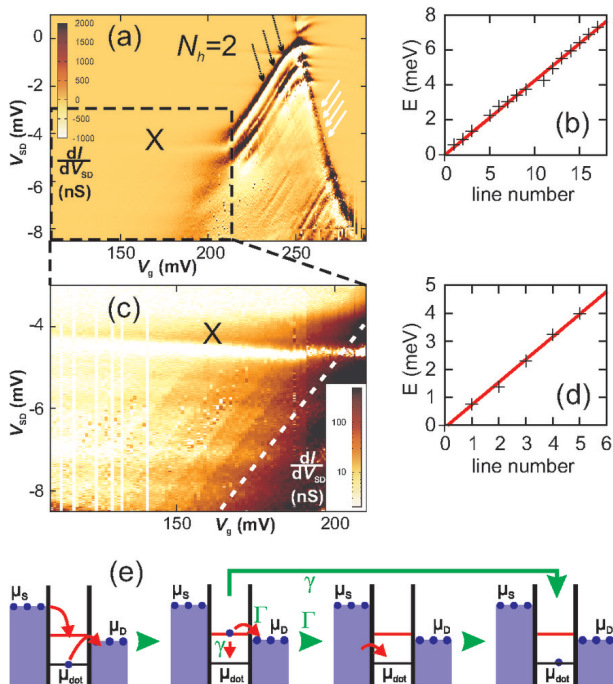


FIG. 2: (Color online) (a) Differential conductance dI/dV_{SD} in the region where the nanotube is charged with $1 \leq N_h \leq 2$ holes, as function of gate voltage V_g and bias voltage V_{SD} (linear color scale). (b) Excitation energies corresponding to the lines of enhanced differential conductance in (a) with positive slope (see white arrows); the x-axis is the line number. The solid line is a linear fit, resulting in an average energy difference of $\Delta E = 0.425 \pm 0.004$ meV per line. (c) Detail zoom of the region marked in (a) with a dashed black line (Coulomb blockade region with $N_h = 2$, logarithmic color scale). A white dashed line sketches the edge of the SET region. (d) Relative excitation energies for the line features in (c), using the same parameters for position to energy conversion. A linear fit results in $\Delta E = 0.810 \pm 0.025$ meV. (e) Schematic detailing cotunnel-assisted sequential tunneling (CO-SET). A prerequisite for the visibility of this process is $\gamma < \Gamma$, i.e. tunnel-out processes dominate in-dot relaxation.

region with $1 \leq N_h \leq 2$ at low negative bias, and the adjacent $N_h = 2$ Coulomb blockade region. A rich spectrum of equidistant excitation lines with positive slope, corresponding to excitations of the $N_h = 1$ system (see e.g. Ref. [16]), is found in SET (white arrows). This is also detailed in Fig. 2(b), which shows the corresponding excitation energies as function of line number

[21]. We assign these excitations to a harmonic vibration whose frequency is $\hbar\omega = 0.425$ meV \pm 0.004 meV, in good agreement with the bulk mechanics prediction of $\hbar\omega_{\text{vib}} = 0.44$ meV for the longitudinal vibration mode of a 250 nm long nanotube segment [7]. In addition, the data of Fig. 2(a) reveals three faint excitation lines with negative slope (i.e. $N_h = 2$ excitations) as well, marked in the color plot by the three black arrows and separated by approximately 0.7 meV. It is difficult to confirm a harmonic spectrum because of the faintness of the three lines and the resulting position error.

Figure 2(c) enlarges the region outlined in Fig. 2(a) by a black dashed rectangle, plotting the differential conductance in logarithmic color scale. Here, Coulomb blockade stabilizes a total charge of $N_h = 2$ holes on the nanotube, suppressing SET. Surprisingly, a pattern of gate dependent excitation lines in the Coulomb blockade region, parallel to the edge of the SET region, emerges as well. Using the same conversion factors between line position and energy as in the SET region, one obtains for these excitations relative energy values as plotted in Fig. 2(d). A regular spacing corresponding to a harmonic oscillator energy of $\hbar\omega = 0.810$ meV \pm 0.025 meV is visible, close to the above mentioned energy scale 0.7 meV of the $N_h = 2$ excitations in SET.

Since these gate dependent lines appear within the Coulomb blockade region of the observed diamond structure in Fig. 2(a), the most straightforward explanation is that they correspond to cotunnel-assisted sequential tunneling (CO-SET) processes [17]. These are multi-step processes, as sketched in Fig. 2(e). Inelastic cotunneling leaves a quantum dot in an excited state (see second panel in the figure), which is possible at any voltage above the energy of this state. Sequential tunneling to the drain electrode can follow for voltages close to the Coulomb diamond edges, even if the Coulomb-blockaded ground state does not allow it. For this to happen, the rate Γ for tunneling out has to be comparable to or larger than the energy relaxation rate γ to the ground state.

In general, CO-SET processes can involve intrinsic (e.g. orbital) excitations of quantum dots as well as vibrational states. Here, as opposed to the measurements of Ref. [17], the highly regular excitation spectrum observed in Fig. 2(c) strongly indicates a vibrational origin. The vibrational CO-SET lines are related to the two-hole charge state vibrational excitations seen in SET with negative slope. As the vibrational energy exceeds thermal broadening ($\hbar\omega \gg k_B T$), the observation of multiple excitations in Coulomb blockade strongly suggests storage and subsequent release of energy in the vibrational mode, involving phonon absorption sidebands [2, 8, 18, 19]. This stands in contrast to the usual assumption that vibrational relaxation is fast and that the mechanical system is predominantly found in its ground state. The required energy is provided by inelastic cotunneling, exciting the vibrational mode and causing its

non-equilibrium occupation.

A particularly interesting feature of the measurement of Fig. 2(a) is that the CO-SET lines can only be observed below a weakly gate-dependent feature of enhanced differential conductance at $V_{SD} \simeq -4$ mV (marked X in the plots); i.e. they only occur at energies higher than 4 meV. This observation is explained by assuming that the line

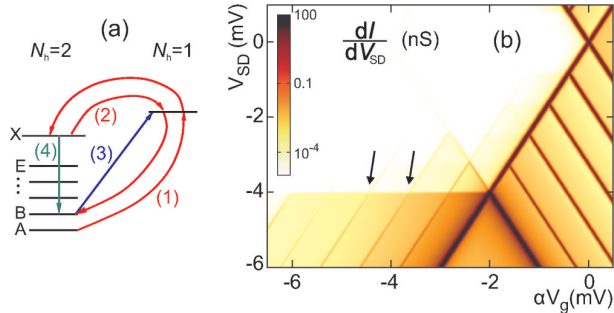


FIG. 3: (Color online) Single quantum dot modeling reproducing the observed transport features: (a) Energy level scheme used in the calculations of (b), as well as the tunneling and relaxation processes relevant for the CO-SET features. (b) Calculated differential conductance as a function of gate voltage V_g and bias voltage V_{SD} , for the following parameters: vibrational level-spacing $\hbar\omega = 810\mu\text{eV}$, $kT = 8.6\mu\text{eV} = 10^3\hbar\Gamma' = 10^4\hbar\gamma' = 10^4\hbar\gamma$. The tunneling couplings were chosen smaller than in the experiment to ensure a well-behaved perturbation expansion. For clarity, V_g has been scaled with the gate conversion factor $\alpha = C_g/C$ [16].

feature marked with X in the measurements represents the onset of an inelastic cotunneling current, corresponding to an electronic excitation of the quantum dot. To understand the resulting interplay between mechanical and electronic excitations we have performed calculations on a simple model system, illustrated in Fig. 3(a). The calculations account for strong Coulomb effects as well as tunneling processes up to 4th order in the tunneling Hamiltonian, responsible for cotunneling, line broadening and level renormalization which are important close to SET resonance, see Ref. [18] for details.

The two-hole ground state and its vibrational excitations are the origin of CO-SET lines as observed in the experiment. To demonstrate this idea, it suffices to consider a model with several equidistant states (A–E), which are assumed to be coupled with the same rate Γ to the one-hole ground state. In addition, a further excited two-hole state (X) supporting a current with rate Γ' is introduced. Since the edge of the Coulomb diamond becomes very broad in the experiment below this excitation, an estimate of the ratio of Γ and Γ' based on the SET current is difficult. However, the strong signature of the inelastic cotunneling line associated with state X indicates that $\Gamma' \gg \Gamma$. The result of a calculation based on this model is shown in Fig. 3(b). The important characteristics of the experiment are reproduced: the signatures of CO-

SET originating from sequential tunneling out of states B–E, process (3) in Figure 3(a), are strongly enhanced below the threshold for inelastic cotunneling connected to state X (see arrows in Fig. 3(b)).

The appearance of a set of harmonic CO-SET lines at high bias can be explained by a subtle interplay of electronic and vibrational excitations, with two possible paths which coexist. For energies larger than the one of the inelastic cotunneling step at $V_{SD} \simeq -4$ mV a two-stage process involving inelastic cotunneling into (process (1)) and out of (process (2)) state X is possible and enhances the population of the vibrational excited states. Thus, while the CO-SET lines can in principle also be present at lower (less negative) bias, below the inelastic cotunneling step they appear considerably more pronounced: the associated rates ($\propto \Gamma\Gamma'$) are much larger than those for populating the excited vibrational states with a single inelastic cotunneling process ($\propto \Gamma^2$) at lower bias. We conclude that the strongly coupled state can pump the vibrational mode out of equilibrium through a sequence of two inelastic cotunneling processes.

The second path that can increase the occupation of states B–E involves direct relaxation of state X (process (4) in Fig. 3(a)) with a rate γ' . This has been included in the model calculations. We have verified that the qualitative result that the CO-SET lines can only be seen below the inelastic cotunneling step connected to state X persists for a wide range of γ' . It is important, though, that the relaxation from states B–E into the two-hole ground state (rate γ) is not too fast ($\gamma \lesssim \Gamma$).

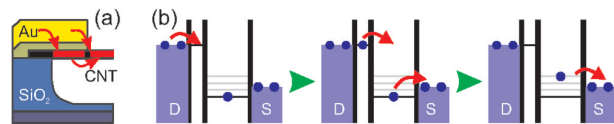


FIG. 4: (Color online) Alternative mechanism for obtaining a vibrational non-equilibrium occupation. (a) Schematic side-view drawing detailing the possible formation of a small quantum dot beneath one of the metallic leads contacting the nanotube. (b) Transport processes for this ‘double quantum dot’ case: additional cotunneling processes are enabled when the small quantum dot enters the energy window given by V_{SD} (see text).

So far we have assumed that the weakly gate-dependent feature X in Fig. 2 corresponds to an electronic *excited* state. An alternative explanation, where the feature corresponds to an electronic *ground* state, leads to an equivalent mechanism for the non-equilibrium occupation of the vibrational mode. The electronic ground state should then originate from a second quantum dot with much weaker gate coupling forming within the nanotube. A possible realization would be the formation of an additional dot beneath one of the contact electrodes as drawn in Fig. 4(a). Indeed, local distortions and curving edges in the measurement of Figs. 1 and 2 may be taken

to hint at several strongly coupled potential minima in the system, as has also been reported in Ref. [20]. Although the number of charges N_h within the suspended nanotube segment remains the same, different gate couplings in the potential minima can lead to ground state transitions and corresponding anticrossings in transport [20].

Fig. 4(b) illustrates the transport process for this ‘double quantum dot’ case. The shielded additional small quantum dot displays a much weaker gate voltage dependence of the level energy. The line of enhanced differential conductance marked in Fig. 2 with X now describes its alignment at the drain lead with the drain Fermi edge. The small quantum dot can then be occupied by a sequential tunneling process as sketched in Fig. 4(b). Inelastic cotunneling through the main dot may follow, leading to the occupation of an excited vibrational state. Although the origin of, and tunneling processes associated with, state X differ from the first scenario, the main effect is the same: state X pumps the vibrational mode through consecutive tunneling events.

A feature of the measurement that has not been discussed so far is that the vibrational frequency in the $N_h = 2$ charge state, as measured both from SET and CO-SET lines, is approximately twice as large as that in the $N_h = 1$ charge state, seen as SET features only. In contrast to previous work on longitudinal phonon excitations in carbon nanotubes [7] the observed quantum dot is in the few-carrier regime. The transition from e.g. one to two trapped holes involves a distinct spatial redistribution of charge along the nanotube [12]. This strongly affects the electrostatic force distribution, which makes variations of vibration mode energies and mode shapes likely. A more detailed theoretical analysis of a coupled system of mechanical oscillator and few interacting localized charges may be merited but surpasses the scope of this Letter.

Finally, the experimental observation of vibrational CO-SET resonances allows to establish a lower boundary for the quality factor of the longitudinal mechanical mode [19], independent of the detailed nature of the pumping mechanism. The tunnel current at the edge of the low-bias CB region ($|V_{SD}| < 4\text{ mV}$), $I \simeq 1\text{ nA}$, provides an approximation for the SET tunneling rate Γ . For the cotunneling-assisted processes to be visible, the lifetime of vibrational excitations must be larger than the corresponding timescale $\tau \simeq 0.16\text{ ns}$. With the vibrational energy $\hbar\omega = 810\text{ }\mu\text{eV}$, one obtains $Q \gtrsim \tau \times \omega/2\pi = 31$. Since we observe several sidebands, a higher value for Q is more likely than this lower boundary, depending on the specific relaxation processes.

In conclusion, we have observed a pattern of equidistant, gate-dependent vibrational excitations *in the Coulomb blocked regime* of a suspended carbon nanotube quantum dot. The appearance of the excitations is explained in the context of co-tunnel assisted se-

quential electron tunneling via phonon absorption processes. Interestingly, the absorption sidebands of the quantized phonon mode are only visible above a high bias voltage threshold. Two models for the enhancement of the non-equilibrium distribution of the mechanical mode are discussed which demonstrate that the mode can be ‘‘pumped’’ either by an electronic excitation of the nanotube, or by a ground-state of another small quantum dot within the same nanotube. The pumping mechanism offers a perspective for electric control of quantized mechanical motion in nanoscale transistors by employing the interplay with electronic degrees of freedom.

The authors would like to thank Yaroslav Blanter and Menno Poot for insightful discussions, and Bert Otte and Hari Pathangi for experimental help. Financial support by the Dutch organization for Fundamental Research on Matter (FOM), the NWO VICI program, NanoNed, DFG SPP-1243, the Helmholtz Foundation, and the FZ-Jülich (IFMIT) is acknowledged.

* Electronic address: mail@akhuettel.de

- [1] S. Braig and K. Flensberg, Phys. Rev. B **68**, 205324 (2003).
- [2] J. Koch, F. von Oppen, and A. V. Andreev, Phys. Rev. B **74**, 205438 (2006).
- [3] A. Mitra, I. Aleiner, and A. J. Millis, Phys. Rev. B **69**, 245302 (2004).
- [4] V. Sazonova, Y. Yaish, H. Ustunel, D. Roundy, T. A. Arias, and P. L. McEuen, Nature **431**, 284 (2004).
- [5] B. Witkamp, M. Poot, and H. van der Zant, Nano Lett. **6**, 2904 (2006).
- [6] B. Reulet, A. Y. Kasumov, M. Kociak, R. Deblock, I. I. Khodos, Y. B. Gorbatov, V. T. Volkov, C. Journet, and H. Bouchiat, Phys. Rev. Lett. **85**, 2829 (2000).
- [7] S. Sapmaz, P. Jarillo-Herrero, Y. M. Blanter, C. Dekker, and H. S. J. van der Zant, Phys. Rev. Lett. **96**, 026801 (2006).
- [8] B. J. LeRoy, S. G. Lemay, J. Kong, and C. Dekker, Nature **432**, 371 (2004).
- [9] M. Bockrath, D. H. Cobden, P. L. McEuen, N. G. Chopra, A. Zettl, A. Thess, and R. E. Smalley, Science **275**, 1922 (1997).
- [10] S. J. Tans, M. H. Devoret, H. Dai, A. Thess, R. E. Smalley, L. J. Geerligs, and C. Dekker, Nature **386**, 474 (1997).
- [11] P. Jarillo-Herrero, S. Sapmaz, C. Dekker, L. P. Kouwenhoven, and H. S. J. van der Zant, Nature **429**, 389 (2004).
- [12] V. V. Deshpande and M. Bockrath, Nature Physics **4**, 314 (2008).
- [13] F. Kueemeth, S. Ilani, D. C. Ralph, and P. L. McEuen, Nature **452**, 448 (2008).
- [14] A. K. Hüttel, M. Poot, B. Witkamp, and H. S. J. van der Zant, New Journal of Physics **10**, 095003 (2008).
- [15] J. Kong, H. T. Soh, A. M. Cassell, C. F. Quate, and H. Dai, Nature **395**, 878 (1998).
- [16] L. P. Kouwenhoven, C. M. Marcus, P. L. McEuen, S. Tarucha, R. M. Westervelt, and N. S. Wingreen, in *Mesoscopic Electron Transport*, edited by L. L. Sohn,

- L. P. Kouwenhoven, and G. Schön (Kluwer, 1997).
- [17] R. Schleser, T. Ihn, E. Ruh, K. Ensslin, M. Tews, D. Pfannkuche, D. C. Driscoll, and A. C. Gossard, Phys. Rev. Lett. **94**, 206805 (2005).
- [18] M. Leijnse and M. R. Wegewijs, Phys. Rev. B (2008), in press; arXiv:0807.4027.
- [19] M. C. Lüffe, J. Koch, and F. von Oppen, Phys. Rev. B **77**, 125306 (2008).
- [20] K. Grove-Rasmussen, H. I. Jørgensen, T. Hayashi, P. E. Lindelof, and T. Fujisawa, Nano Letters **8**, 1055 (2008).
- [21] No clear features can be identified in the data at the positions expected for lines 4 and 10. This may e.g. be due to electronic transitions shadowing the vibrational effects in transport.